Axially graded heteroepitaxy and Raman spectroscopic characterizations of Si 1 − x Ge x nanowires

Jee-Eun Yang, Won-Hwa Park, Cheol-Joo Kim, Zee Hwan Kim, and Moon-Ho Jo

Articles you may be interested in

Anomalous junctions characterized by Raman spectroscopy in Si x Ge1− x nanowires with axially degraded components
Appl. Phys. Lett. **105**, 101902 (2014); 10.1063/1.4895515

Band engineered epitaxial Ge – Si x Ge 1 − x core-shell nanowire heterostructures
Appl. Phys. Lett. **95**, 033101 (2009); 10.1063/1.3173811

Raman characterization of Ge distribution in individual Si 1 − x Ge x alloy nanowires
Appl. Phys. Lett. **93**, 203101 (2008); 10.1063/1.3028027

Raman and electron microscopic studies of Si 1 − x Ge x alloy nanowires grown by chemical vapor deposition
J. Appl. Phys. **102**, 124307 (2007); 10.1063/1.2817619

β - Ga 2 O 3 nanowires: Synthesis, characterization, and p -channel field-effect transistor
Appl. Phys. Lett. **87**, 222102 (2005); 10.1063/1.2135867

Axially graded heteroepitaxy and Raman spectroscopic characterizations of $Si_{1-x}Ge_x$ nanowires

Jee-Eun Yang,[1] Won-Hwa Park,[2] Cheol-Joo Kim,[1] Zee Hwan Kim,[2,a)] and Moon-Ho Jo[1,b)]

[1]*Department of Materials Science and Engineering, Pohang University of Science and Technology (POSTECH), San 31, Hyoja-Dong, Nam-Gu, Pohang, Gyungbuk 790-784, Republic of Korea*
[2]*Department of Chemistry, Korea University, Anam-Dong, Seongbuk-Gu, Seoul 136-701, Republic of Korea*

We report the axially graded heteroepitaxy of $Si_{1-x}Ge_x$ nanowires, by the kinetic controls of the Au-catalytic decomposition of precursors during chemical vapor syntheses. Transmission electron microscope studies demonstrate that the relative composition of Si and Ge is continuously graded along the uniformly thick nanowires, sharing the same crystal structures with the continuously varying lattices. We also employed a confocal Raman scattering imaging technique, and showed that the local variations in Raman phonon bands, specific to Si and Ge alloying (ν_{Si-Si}, ν_{Si-Ge}, and ν_{Ge-Ge}), can be spatially and spectrally resolved along the individual nanowires, within the spatial resolution of ~500 nm. © *2008 American Institute of Physics*. [DOI: 10.1063/1.2939564]

Optical and electrical properties of semiconductors at the nanometer regime manifest themselves to be strongly size dependent, and such substantial variations have been intensively investigated in nanoscale science and technology as central research themes.[1] For example, optical quantum confinements, often observed from various semiconductor nanocrystals, offer challenging opportunities for their applications into photonics and biomedicine as optically active components. Yet, the optical characterizations of such size-dependent variation are not readily available with an ensemble of nanocrystals, due to the statistical averaging arising from the finite size distributions of constituent nanocrystals. In this respect it is empirically required to optically characterize either on an individual nanocrystal whose size and geometry are precisely defined, or on the specimen of the collections of size-homogeneous nanocrystals, which is then practically difficult to achieve. Here we report the axially graded heteroepitaxy and a confocal Raman scattering imaging of an individual one-dimensional $Si_{1-x}Ge_x$ alloy crystal,[2–4] where the relative composition of Si and Ge is continuously modulated in a wide range along the individual nanowires, sharing the same crystal structures with the continuously varying lattices. The optical properties of $Si_{1-x}Ge_x$ nanowires are particularly interesting, because they can provide unique opportunities to investigate both the alloying and size effects at the nanometer scale on their energy-band gaps at the same time.[2,5] On-wire, composition- and lattice-modulated $Si_{1-x}Ge_x$ alloy nanowires in our study thus can represent as a model system of continuously energy-band gaps within a well defined size and dimension for the size-dependent optical properties.[2,6] Specifically, we show that, by the kinetic controls of the catalytic decomposition SiH_4 and GeH_4 precursors during Au-catalytic chemical vapor syntheses, the relative composition of Si and Ge can be continuously tuned along the uniformly thick (20–30 nm) nanowires in the same crystal structures against the general tendency toward phase segregations in bulk crystals.[7] By employing a confocal Raman scattering imaging technique done on individual $Si_{1-x}Ge_x$ nanowires, we also demonstrate

that the local variations in compositions can be spatially and spectrally resolved along the individual nanowires. The spatially resolved spectra of the Raman phonon bands (ν_{Si-Si}, ν_{Si-Ge}, or ν_{Ge-Ge}) allow us to optically estimate the local composition along the wire axis within the 500 nm spatial resolution.

Single-crystalline $Si_{1-x}Ge_x$ nanowires in our study were synthesized by Au catalyst-assisted chemical vapor syntheses, as schematically specified in Fig. 1(a).[2,8,9] We start off with the preparation of Au catalysts of the nanometer scale by deposition of very thin Au films or dispersion of colloidal Au nanoparticles on SiO_2/Si (100) or quartz substrates. Subsequently, the chemical vapor syntheses was carried out under a varying flow of independent SiH_4 and GeH_4 precursors (specifically, 10% of SiH_4 and GeH_4 premixed in H_2) at given temperatures and pressure. We attempted the on-wire combinatorial growth approaches by modulating the flow rate of SiH_4 and GeH_4 in a given growth time with the values extracted from the independent growth kinetics of individual Si and Ge nanowires. Specifically, during the first 180 s, we inlet only GeH_4 to grow pure Ge nanowire segments, and later introduced SiH_4 in addition at the constant temperature and pressure. The flow rate of two precursor was tuned for every 40 s and only SiH_4 was maintained in the last 180 s. There is a general tendency that the nanowires are tapered under the GeH_4 rich conditions due to the faster thermal decomposition kinetics of GeH_4 compared to that of SiH_4. Thus we have paid particular attention to maintain the uniform nanowire diameters along the entire axis without tapering by Ge radial growth.[8] For that we have optimized the growth conditions, such as the growth temperature of 390 °C, the total gas pressure of 200 Torr with introducing H_2 gases to effectively suppress the radial growth.

Figures 1(b)–1(d) are the representative transmission electron microscope (TEM) images of an individual $Si_{1-x}Ge_x$ nanowire of 20 nm in diameter. The observation of Au catalysts at the front tip of the nanowires, as in Fig. 1(b), suggests that nanowire growth is governed by the vapor-liquid-solid mechanism.[10,11] The high resolution TEM images and diffraction patterns along the nanowire also demonstrated that the nanowires are single crystalline with the same crystal orientation along the entire nanowire length. The nanowires in Fig. 1 grow in the [011] direction along the entire length

a)Electronic mail: zhkim@korea.ac.kr.
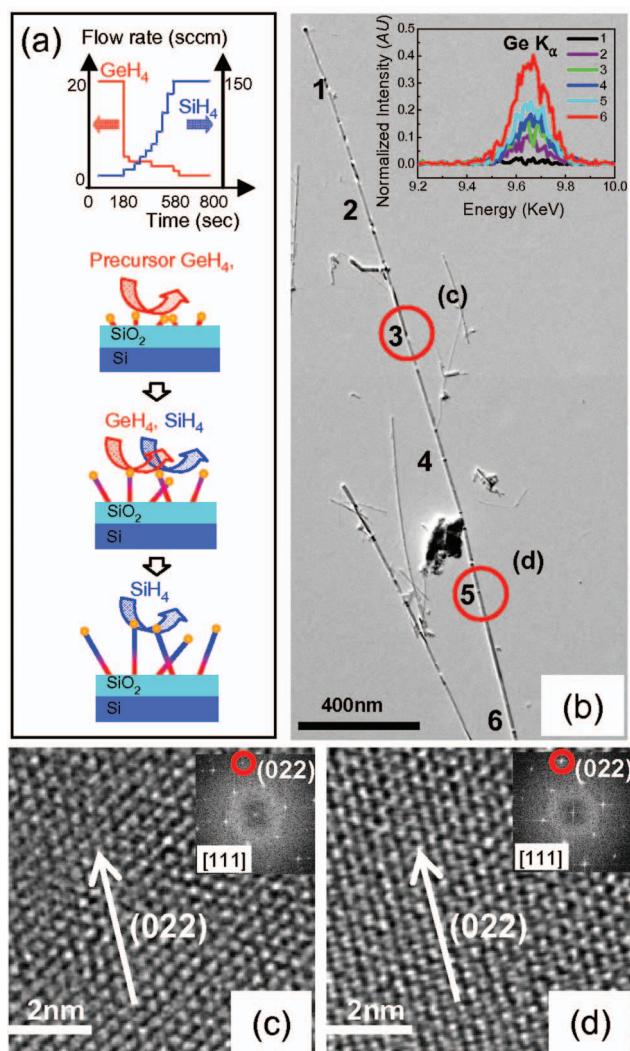b)Electronic mail: mhjo@postech.ac.kr.

FIG. 1. (Color) (a) The schematics of our combinatorial syntheses; the flow rates of GeH_4 and SiH_4 were systematically modulated for the total growth of 800 s. (b) A representative TEM image of an individual $Si_{1-x}Ge_x$ nanowire. Inset shows the intensity of Ge $K\alpha$ radiations in energy-dispersive ray EDX spectra collected from six different positions (1–6) marked in (b). The intensity of all spectra was normalized respect to Si $K\alpha$ radiation for comparison. (c)–(d) High resolution TEM images of the nanowire at different positions marked in (b). Insets are electron diffraction patterns indicating that the crystal orientation along the length is [211].

FIG. 2. (Color) The Ge contents and {022} interplanar distances at six different positions of an individual $Si_{1-x}Ge_x$ nanowire, marked in Fig. 1(b). Open circles are {022} interplanar distances in the bulk limit, extracted from the measured compositions. The inset schematically indicates that some degree of strain, associated with the graded axial heteroepitaxy of Si on Ge, is built up within the individual nanowire due to the lattice mismatch.

direction, although it was found that the crystal orientation along the growth direction varies for the nanowires of different diameters.[12] The axial variation in the relative composition of Si and Ge along the nanowires is determined from the energy dispersive x-ray (EDX) spectra by the convergent electron beam in TEM. Figure 1(b) inset shows the variation in the normalized intensity of Ge $K\alpha$ radiations with respect to those of Si $K\alpha$ radiations, probed on individual nanowires along the marked positions spaced by ∼400 nm in Fig. 1(b). The systematic variation in the Ge content suggests that the appropriate alloying of Si and Ge is reproducibly tuned by the kinetic control of the catalytic decomposition SiH_4 and GeH_4 precursors. Quantitative analyses on the relative compositions and lattices along the individual $Si_{1-x}Ge_x$ nanowire of Fig. 1 were summarized in Fig. 2. We immediately find that the relative composition of Ge linearly decreases as the position moves toward the Au catalysts, as expected from the growth sequence. In a same fashion, it is also found that the interplanar distance of {022} planes, which stacks along the
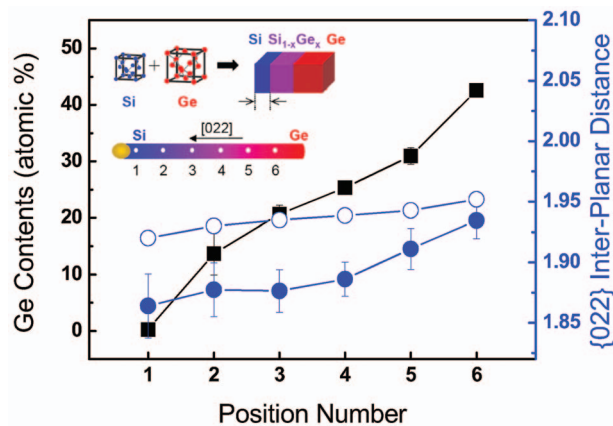
wire axis, systematically decreases. Notably, when the Si content increases nearer the catalysts, these {022} planar distance, parallel to the [022] growth direction, decrease more steeply than those extracted from the measured composition, which thus represent the values in the bulk limit. We speculate that some degree of strain, associated with the graded axial heteroepitaxy of Si on Ge, is built up within the individual nanowire due to the lattice mismatch, as schematically represented in the inset. This finding, in return, assures the high degree of the continuously graded heteroepitaxy of Si and Ge, which is not readily available in the counterparts of thin film heteroepitaxy.

In order to further investigate the local variations in compositions by optical characterizations, we carried out the confocal Raman microscopic and spectroscopic measurements on individual $Si_{1-x}Ge_x$ nanowires. Specifically, we employed an epiconfocal Raman microscope equipped with a linearly polarized 532 nm excitation light source [Nd: YAG (neodymium-doped yttrium aluminum garnet) laser] and a spectrograph (a monochromator and a TE-cooled charge-coupled device camera). Figures 3(e) and 3(f) display Stokes-shifted Raman spectra collected from marked positions (A and B) along the nanowire axis in the Fig. 3(a), together with a Raman spectrum of the bulk Si wafer in Fig. 3(g) as a frequency reference. The three peaks in the spectra corresponds to the lattice phonon vibration modes of Si–Si (ν_{Si-Si}, ∼500 cm^{-1}), Si–Ge (ν_{Si-Ge} ∼400 cm^{-1}), and Ge–Ge (ν_{Ge-Ge} ∼270 cm^{-1}) bonds[13,14] of the nanowires. The corresponding Raman images of the identical $Si_{1-x}Ge_x$ nanowire in Figs. 3(b)–3(d) show the monitoring of the respective phonon bands. The observed Raman spectra bear close similarity in both peak positions and spectral widths to those of the bulk $Si_{1-x}Ge_x$ alloys and $Si_{1-x}Ge_x$ nanoparticles with varying degrees of Ge concentrations.[15] We recognize that the relative intensities of ν_{Si-Si} versus ν_{Ge-Ge} peaks smoothly change as we move along the nanowire without any discontinuity or discrete domains, indicating the continuous compositional variation along the SiGe nanowire within our optical resolution of ∼500 nm. We also observe continuous distribution of the ν_{Si-Ge} intensity along the entire length of the nanowire in the image, which confirms that the homogeneous alloying persists throughout the entire nanowire (note that the phase-
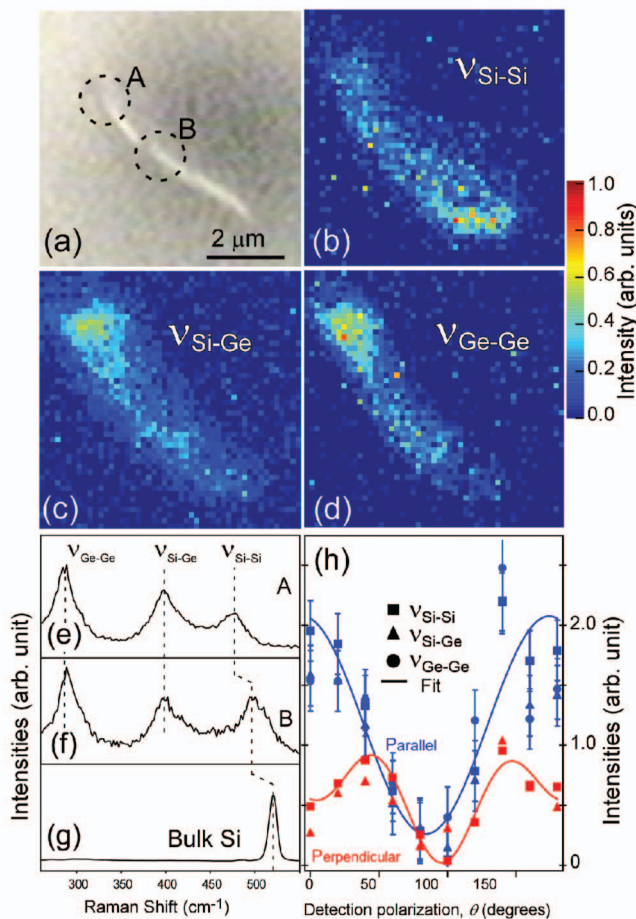
FIG. 3. (Color) (a) Optical micrograph of a $Si_{1-x}Ge_x$ nanowire under Raman characterizations. Confocal Raman images of $Si_{1-x}Ge_x$ nanowire obtained by integrating ν_{Si-Si} (b), ν_{Si-Ge} (c), and ν_{Ge-Ge} (d) Raman transitions. Typical Raman spectra obtained at the point A (e) and B (f) of the $Si_{1-x}Ge_x$ nanowire, and bulk Si (g), along with the band assignment. The color scale on the Raman images is normalized in order to show the detailed intensity variations. (h) Raman band intensities plotted as a function of detection polarization for parallel and perpendicular polarization excitations. The squares, triangles, and circles represent the ν_{Si-Si}, ν_{Si-Ge}, and ν_{Ge-Ge} bands respectively. The solid line corresponds to the fit. The ν_{Ge-Ge} signal for perpendicularly polarized excitation is not included because of poor signal/noise ratio. The error bars represent the instrumental noise within spectral integration.

segregated SiGe nanowires will not show Si–Ge phonon mode in the Raman spectra). Upon close examination of the Raman spectra, we also notice the systematic frequency change in the ν_{Si-Si} transition with the change in the local Ge concentration, which is consistent with the earlier observations in $Si_{1-x}Ge_x$ nanospheres and bulk $Si_{1-x}Ge_x$ alloys.[14] With the assumption that the $Si_{1-x}Ge_x$ nanowire follows the same frequency shift/Ge-concentration rule as empirically found in the bulk and nanospheres,[4] we estimate that the local concentrations of the Ge at the positions of A and B to be 0.64 and 0.33, respectively.

It is generally accepted that Raman scattering of semiconductor nanowires depends on the excitation and detection polarizations. These anisotropies originate both from the

crystal orientation[15] (Raman tensor depends on the crystal symmetry) and/or from the polarization-dependent mesoscopic radiative coupling of the excitation radiation onto the cylindrically shaped nanowire axis.[16] From all three phonon bands of (ν_{Si-Si}, ν_{Si-Ge}, or ν_{Ge-Ge}), we consistently observe about 2:1 of Raman intensity ratio between the excitation polarization aligned parallel and perpendicular to the nanowire axis from all of the $Si_{1-x}Ge_x$ nanowires we have examined. In addition, the Raman scattered radiation is strongly polarized along the nanowire axis irrespective of the phonon bands, all of which could be fitted with $I = I_0 + I_1 \cos^2 \theta + I_2 \cos^2 2\theta$ (where the θ is the angle between the nanowire axis and the detection polarization direction, and I_0, I_1, I_2 are the fitting coefficients, and $\theta = 0°$ corresponds to the nanowire axis with respect to the detection polarization), as shown in Fig. 3(h). This ensures that our Raman spectra and images taken with a particular excitation polarization do not bias a particular phonon mode of the $Si_{1-x}Ge_x$ nanowires.

[1] A. P. Alivisatos, Science **271**, 933 (1996).
[2] J.-E. Yang, C.-B. Jin, C.-J. Kim, and M.-H. Jo, Nano Lett. **6**, 2679 (2006).
[3] X. F. Duan and C. M. Lieber, Adv. Mater. (Weinheim, Ger.) **12**, 298 (2000) and K. K. Lew, L. Pan, E. C. Dickey, and J. M. Redwing, *ibid.* **15**, 2073 (2003).
[4] H. Takagi, H. Ogawa, Y. Yamazaki, A. Ishizaki, and T. Nakagiri, Appl. Phys. Lett. **56**, 2379 (1990); S. Schuppler, S. L. Friedman, M. A. Marcus, D. L. Adler, Y.-H. Xie, F. M. Ross, T. D. Harris, W. L. Brown, Y. J. Chabal, L. E. Brus, and P. H. Citrin, Phys. Rev. Lett. **72**, 2648 (1994); T. van Buuren, L. N. Dinh, L. L. Chase, W. J. Siekhaus, and L. J. Terminello, *ibid.* **80**, 3803 (1998).
[5] T. Kuykendal, P. Ulich, S. Aloni, and P. Yang, Nat. Mater. **6**, 951 (2007).
[6] D. C. Ahlgren and J. Dunn, *JBM MicroNews* (IBM Microelectronics, Vermont, 2000) 6, 1 and J. Ouellette, *The Industrial Phycsicist* (American Institute of Physics, New York, 2002).
[7] M. I. Alonso and K. Winer, Phys. Rev. B **39**, 10056 (1989); M. Franz, K. F. Dombrowski, H. Rucker, B. Dietrich, and K. Pressel, *ibid.* **59**, 10614 (1999); Z. F. Sui, H. H. Burke, and I. P. Herman, *ibid.* **48**, 2162 (1993).
[8] C.-B. Jin, J.-E. Yang and M.-H. Jo, Appl. Phys. Lett. **88**, 193105 (2006).
[9] C.-J. Kim, W.-H. Park, J.-E. Yang, H.-S. Lee, S. Maeng, Z. H. Kim, H. M. Jang, and M.-H. Jo, Appl. Phys. Lett. **91**, 033104 (2007).
[10] R. S. Wagner and W. C. Eliis, Appl. Phys. Lett. **4**, 89 (1964).
[11] A. M. Morales and C. M. Lieber, Science **279**, 208 (1998).
[12] Y. Wu, Y. Cui, L. Huynh, C. J. Barrelet, D. C. Bell, and C. M. Lieber, Nano Lett. **4**, 433 (2004).
[13] S. Takeoka, K. Toshikiyo, M. Fujii, S. Hayashi, and K. Yamamoto, Phys. Rev. B **61**, 15988 (2000).
[14] Z. Sui, H. H. Burke, and I. P. Herman, Phys. Rev. B **48**, 2162 (1993).
[15] P. J. Pauzauskie, D. Talaga, K. Seo, P. Yang, and F. Lagugne-Labarthet, J. Am. Chem. Soc. **147**, 17146 (2005).
[16] J. Frchette and C. Carraro, Phys. Rev. B **74**, 161404 (2006).